JOURNAL OF Materials CHEMISTRY

Luminescent properties of $BaMg_2Si_2O_7$:Eu^{2+},Mn^{2+}†

G. Q. Yao, J. H. Lin, L. Zhang, G. X. Lu, M. L. Gong and M. Z. Su

State Key Laboratory of Rare Earth Materials Chemistry and Applications, Department of Materials Chemistry, 317 Chemistry Hall, Peking University, Beijing 100871, P. R. China

Pure $BaMg_2Si_2O_7$, and its europium and magnesium doped forms, have been synthesized by solid state reaction. $BaMg_2Si_2O_7$ and $BaMn_2Si_2O_7$ crystallize in an orthorhombic structure with the space group *Ama*2. The lattice constants obtained from X-ray powder diffraction are $a=13.742(2)$ Å, $b=12.698(2)$ Å and $c=7.237(1)$ Å for $BaMg_2Si_2O_7$ and $a=14.030(2)$ Å, $b=12.941(1)$ Å and $c=7.285(1)$ Å for $BaMn_2Si_2O_7$. The emission spectra of the Eu^{2+} and Mn^{2+} doped $BaMg_2Si_2O_7$ materials appear as broad bands peaking at 400 and 690 nm respectively. The luminescent studies performed on the samples with different doping concentrations suggest that the $Eu^{2+} \rightarrow Mn^{2+}$ energy transfer takes place in the doubly doped samples.

Introduction

Mn^{2+} doped luminescent materials have been known to show wide-ranging emission, from 500 nm to 700 nm, depending upon the crystal field of the host materials. Many luminescent materials, particularly those used in fluorescent lamps, have been developed based on the interesting properties of Mn^{2+}. However, the Mn^{2+} emission intensity under UV excitation, in general, is low if materials are doped only with Mn^{2+}. The reason for this phenomenon is that nearly all of the optical transitions, from the near ultraviolet to the visible range, are parity or spin forbidden. Sensitizers, therefore, have to be employed in Mn^{2+} doped materials. It is known that Eu^{2+}, as a promising sensitizer, provides efficient energy transfer to Mn^{2+} in some host materials.[1–3] Caldino *et al.*[2,3] have studied the energy transfer between Eu^{2+} and Mn^{2+} in $CaCl_2$ and indicated that effective energy transfer can be understood by the formation of Eu–Mn complexes. The Eu–Mn complexes may only be present in host materials like $CaCl_2$, since the elastic strain induced by the doped ions is minimized by the complexes. Many years ago Barry[1] studied europium and manganese co-doped $BaMg_2Si_2O_7$ and observed effective energy transfer from Eu^{2+} to Mn^{2+}. As far as the ionic size is concerned, Eu^{2+} ions should occupy the Ba^{2+} sites, while the Mg^{2+} sites are preferred for the Mn^{2+} ions, so this material is a suitable candidate for energy transfer between the randomly distributed Eu^{2+} and Mn^{2+}. However, the structure of $BaMg_2Si_2O_7$ was not known and the energy transfer between Eu^{2+} and Mn^{2+} in $BaMg_2Si_2O_7$ has not yet been fully studied.

Since the optical absorption of Eu^{2+} originates from the allowed transition between 4f and 5d, further study of the energy transfer between Eu^{2+} and Mn^{2+} may be helpful in developing new efficient luminescent materials with a wide variety of colors. In this paper we present our recent study on the structure and the luminescent properties of Eu^{2+} and Mn^{2+} in $BaMg_2Si_2O_7$. Based on the concentration dependence of the luminescent intensity and the variations of the decay time of Eu^{2+}, we will address the interaction between Eu^{2+} and Mn^{2+} during the energy transfer.

Experimental

The phosphors with the general formula $Ba_{1-x}Eu_xMg_{2-y}Mn_ySi_2O_7$ were prepared by solid state reaction at high temperature. The stoichiometric starting materials, *i.e.* $BaCO_3$, $MgC_2O_4 \cdot 2H_2O$, Eu_2O_3, $MnCO_3$ and SiO_2, were thoroughly mixed and heated at 1035 °C in a slightly reducing atmosphere of carbon oxide for 4 h. The final products were all single phases and appeared as white crystalline powders.

X-Ray powder diffraction was carried out with a Rigaku D/max-2000 powder diffractometer with Cu-Kα radiation and electron diffraction was studied with a 200CX TEM. The luminescence spectra were recorded with a Hitachi 850 fluorescence spectrophotometer and were all corrected for the lamp output and the photomultiplier. The decay times were measured with a SLM-48000 multi-frequency lifetime fluorometer and the frequency used in the measurement ranged from 2 kHz to 2 MHz. A glycogen–water suspension was used as the lifetime reference and the decay times and decay curves were extracted from both phase differences and de-modulation at different frequencies with least-squares methods.[4]

Results and Discussion

Structure of $BaMg_2Si_2O_7$ and $BaMn_2Si_2O_7$

Fig. 1 shows X-ray powder diffraction patterns of $BaMg_2Si_2O_7$ and $BaMn_2Si_2O_7$. The diffraction pattern of $BaZn_2Si_2O_7$ is also included for comparison. All of these compounds crystallize in an orthorhombic structure with unit cells of $a=13.742(2)$ Å, $b=12.698(2)$ Å and $c=7.237(1)$ Å for $BaMg_2Si_2O_7$ and $a=14.030(2)$ Å, $b=12.941(1)$ Å and $c=7.285(1)$ Å for $BaMn_2Si_2O_7$. The space groups derived from both electron diffraction and X-ray powder diffraction are *Amam*, $A2_1am$ or *Ama*2. Recently we have established the

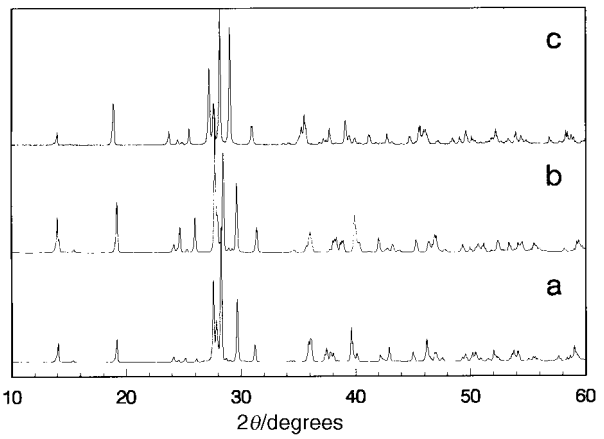

Fig. 1 X-Ray powder diffraction patterns of (a) $BaZn_2Si_2O_7$, (b) $BaMg_2Si_2O_7$ and (c) $BaMn_2Si_2O_7$

† Presented at the Third International Conference on Materials Chemistry, MC^3, University of Exeter, 21–25 July 1997.

crystal structure of $BaZn_2Si_2O_7$ by direct methods from X-ray powder diffraction data, which will be published elsewhere.[5] From the X-ray diffraction patterns, it can be seen that $BaMg_2Si_2O_7$ and $BaMn_2Si_2O_7$ are isostructural with $BaZn_2Si_2O_7$. Fig. 2 presents a projection of the $BaZn_2Si_2O_7$ structure along the *c*-axis. The space group of $BaZn_2Si_2O_7$ is *Ama*2 and its structure consists of polysilicate ions, $Si_2O_7^{6-}$. The zinc atoms are coordinated by five oxygen atoms and barium atoms are coordinated by seven oxygen atoms. In $BaMg_2Si_2O_7$ and $BaMn_2Si_2O_7$, the magnesium and manganese atoms should be located at the zinc positions and they form a complete solid solution as shown in Fig. 3.

Luminescent properties

$Ba_{1-x}Mg_2Si_2O_7$:xEu^{2+}. As far as the ionic radii and the coordination preference are concerned, the doped Eu^{2+} ions should occupy the Ba^{2+} sites in $BaMg_2Si_2O_7$. The excitation and emission spectra of $BaMg_2Si_2O_7$:Eu^{2+}, shown in Fig. 4, are all broad bands peaking at 300 nm and 400 nm respectively. These bands originate from the transition between $^8S_{7/2}$ and $4f^65d^1$. Blasse[6] has summarized the 5d–4f transition in different hosts and pointed out that the position of the lowest excitation state of Eu^{2+} depends strongly on the local environment. If the crystal field is weak, $4f^65d^1$ shifts to high energy so that the $^6P_{7/2}$ level of the $4f^7$ configuration will stay below it, resulting in a sharp $^6P_{7/2}\rightarrow{}^8S_{7/2}$ transition in the emission spectrum. In the case of $BaMg_2Si_2O_7$:Eu^{2+} only the $4f^65d^1\rightarrow{}^8S_{7/2}$ transition is observed, so that $4f^65d^1$ should remain as the lowest excitation state.

The emission intensity of Eu^{2+} in $Ba_{1-x}Eu_xMg_2Si_2O_7$, which depends strongly on the Eu^{2+} concentration as shown in Fig. 5, increases with the Eu^{2+} concentration up to $x=0.006$ and then decreases gradually as the concentration goes higher. The decay of Eu^{2+} emission in this material, obtained with the phase-modulation method, can be represented very nicely with the single exponential expression $[I=I_0\exp(-t/\tau)]$. Meanwhile the decay time τ of Eu^{2+} decreases constantly with the increase of Eu^{2+} concentration. The single exponential decay of the Eu^{2+} emission means either that the luminescence center is well isolated or that excitation energy migrates between the same kind of luminescence centers.[7] Because of the significant overlap between the excitation and emission spectra, effective energy migration between the europium atoms is expected for $Ba_{1-x}Eu_xMg_2Si_2O_7$. However, the energy migration rate may not be very high when the Eu^{2+} concentration is lower than $x=0.006$.

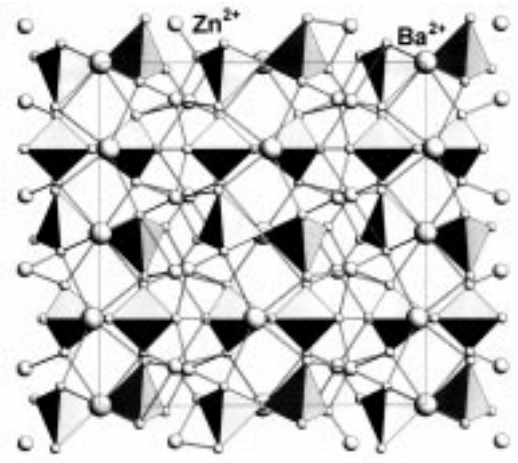

Fig. 2 Crystal structure of $BaZn_2Si_2O_7$ projected along the *c*-axis

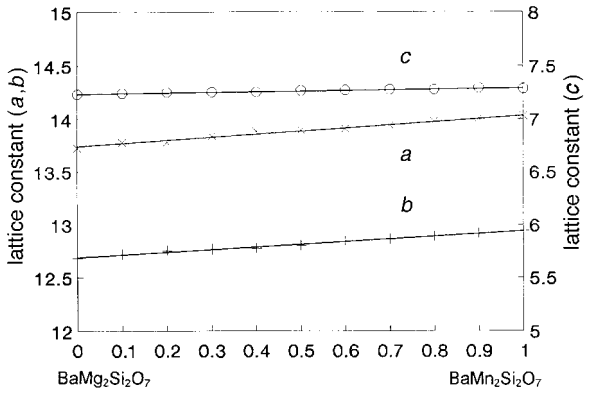

Fig. 3 Lattice constants of the $BaMg_{2-x}Mn_xSi_2O_7$

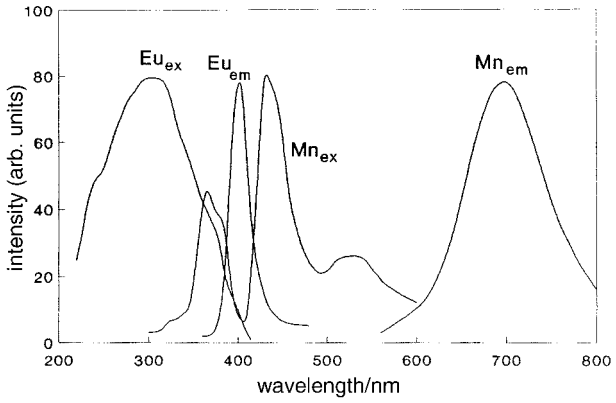

Fig. 4 Excitation and emission spectra of $BaMg_2Si_2O_7$:Eu^{2+} and $BaMg_2Si_2O_7$:Mn^{2+}

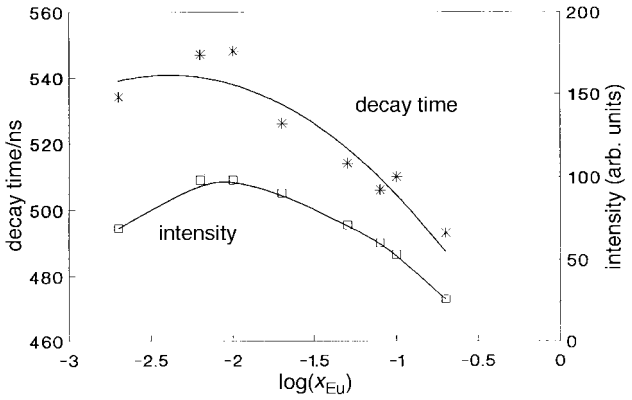

Fig. 5 Concentration dependence of emission intensity and decay time of Eu^{2+} in $BaMg_2Si_2O_7$:xEu^{2+}

$BaMg_{2-y}Si_2O_7$:yMn^{2+}. In Fig. 4 we also show the excitation and emission spectra of Mn^{2+} doped $BaMg_2Si_2O_7$. Considering the ionic sizes, the Mn^{2+} should substitute in magnesium positions in $BaMg_2Si_2O_7$. Fig. 6 shows the intensity and wavelength of Mn^{2+} emission in this material. The emission peak of Mn^{2+} in $BaMg_2Si_2O_7$ shows a red-shift from 614 nm to 690 nm as the concentration increases from 0.001 to 0.1 and it remains at this saturation value at higher concentrations. As far as the ionic radii of Mn^{2+} (0.89 Å) and Mg^{2+} (0.80 Å) are concerned, the Mn–O distance should be larger at higher substitution levels than at lower levels and this leads to a reduction of the crystal field as the doping concentration increases. According to the Tanabe–Sugano diagram for d^5 ions, a blue-shift of the Mn^{2+} emission is expected in $BaMg_2Si_2O_7$:Mn^{2+} on decreasing the crystal field. However, a red-shift of the Mn^{2+} emission has also been observed in $ZnSiO_4$:Mn and interpreted recently by considering the exchange interaction between Mn^{2+} ions.[8] It seems,

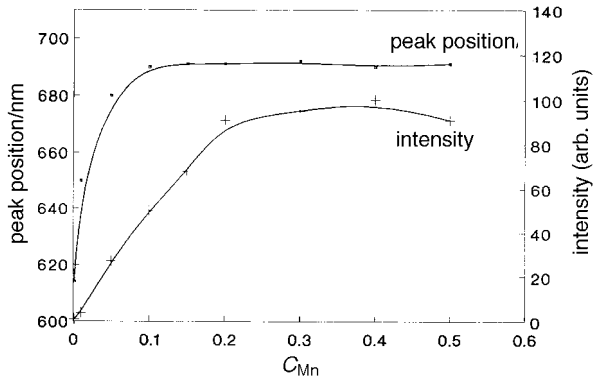

Fig. 6 Concentration dependence of the emission peak position and intensity of $BaMg_2Si_2O_7$:xMn^{2+}

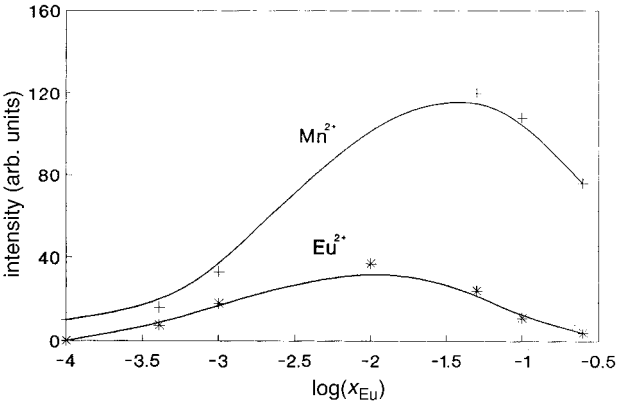

Fig. 8 Concentration dependence of emission intensity of Eu^{2+} and Mn^{2+} in the first series of $BaMg_2Si_2O_7$:xEu^{2+},0.2Mn^{2+} (see text)

therefore, that the exchange interaction between the Mn^{2+} ions plays a significant role in the luminescence of $BaMg_2Si_2O_7$:Mn^{2+}.

$Ba_{1-x}Mg_{2-y}Si_2O_7$:xEu^{2+},yMn^{2+}. From Fig. 4 one can see a significant spectral overlap between the emission of Eu^{2+} and the excitation of Mn^{2+}, therefore effective energy transfer from Eu^{2+} to Mn^{2+} is expected for the co-doped samples. Fig. 7 shows the excitation spectrum monitored by Mn^{2+} emission, in which one can clearly see the Eu^{2+} excitation bands. To understand the energy transfer between Eu^{2+} and Mn^{2+} in $BaMg_2Si_2O_7$, two series of samples were prepared. In the first series, Mn^{2+} was fixed at $y=0.2$ and the doping concentration of Eu^{2+} was varied from $x=0.0$ to 0.20. In another series, the concentration of Mn^{2+} varies from $y=0$ to 0.5, while the Eu^{2+} concentration was fixed at $x=0.006$. For all the co-doped samples, the emission spectra consist of the emission bands of Eu^{2+} and Mn^{2+}, but their intensities strongly depend on the doping concentration. Fig. 8 shows the variation of the emission intensities of Eu^{2+} and Mn^{2+} of the first series. Although the Mn^{2+} concentration was fixed at $y=0.2$, a great enhancement of the Mn^{2+} emission is observed when the concentration of Eu^{2+} increases, indicating significant energy transfer from Eu^{2+} to Mn^{2+}. At low Eu^{2+} concentration, the emission intensities of both Eu^{2+} and Mn^{2+} increase with the increase of the Eu^{2+} concentration. At $x=0.01$ the emission intensity of Eu^{2+} starts to decline, while that of Mn^{2+} is still enhanced up to $x=0.05$. In these samples one has to consider two different types of energy transfer, *i.e.* the energy migration within the Eu^{2+} ions and the energy transfer from Eu^{2+} to Mn^{2+}. When the concentration of Eu^{2+} is lower than 0.001, the emission intensity of Mn^{2+} remains almost constant, indicating that no effective energy transfer happened. Further increase of the Eu^{2+} concentration results in a great enhancement of the Mn^{2+} emission. So the energy transfer between Eu^{2+} and Mn^{2+} seems to be dominant in the range of $x=0.001$ to 0.05. The energy transfer between the Eu^{2+} ions becomes more important when the concentration of Eu^{2+} is greater than 0.05, so that the emission intensities of both Eu^{2+} and Mn^{2+} decrease in the high concentration range.

Fig. 9 shows the emission intensities of Eu^{2+} and Mn^{2+} in the second series. The emission of Eu^{2+} decreases dramatically with increasing Mn^{2+} concentration. At the same time, a significant enhancement of the Mn^{2+} emission is observed. From the structure of $BaMg_2Si_2O_7$, it is known that the distance between Ba and Mg varies from 370 pm to 450 pm, so it seems likely that the energy transfer between Eu and Mn is through the exchange interaction. Flint *et al.*[9–11] proposed a shell model which could account for the energy transfer in crystalline materials, particularly for highly doped materials. If the material crystallizes in high symmetry, the decay of the luminescence can be obtained in a straightforward way from the shell model. In the structure of $BaMg_2Si_2O_7$, all of the barium atoms are located at low symmetry positions and the distances from Ba^{2+} to the eight nearest Mg^{2+} ions are different, ranging from 370 pm to 450 pm. It is therefore difficult to calculate the decay curve of Eu^{2+} directly from structure parameters and the shell model. However, the decay of the Eu^{2+} in this series can be represented by a multiple-exponential function. Fig. 10 shows the decay curves of these samples produced by fitting the phase-difference and demodulation at different frequencies. One can see that the decay of the europium doped sample can be expressed as a single-exponential function with a decay time of $\tau_0=548$ ns. This is the radiative decay time of the Eu^{2+}. For the samples doped with Eu^{2+} and Mn^{2+}, the decay curves deviate from a single exponential function, and can be expressed with a multiple-

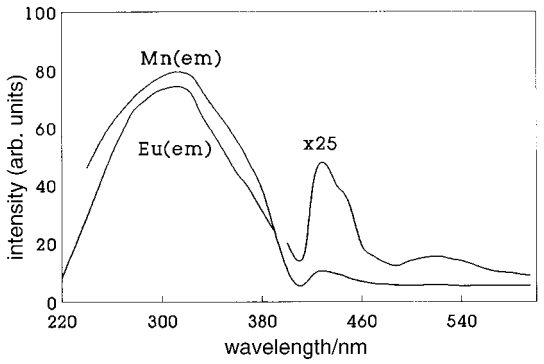

Fig. 7 Excitation spectra monitored by the Mn^{2+} and Eu^{2+} emissions in $BaMg_2Si_2O_7$:Eu^{2+},Mn^{2+}

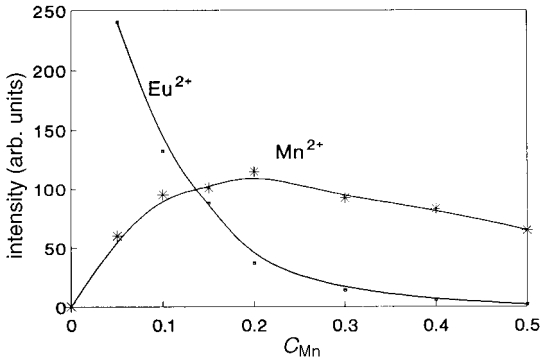

Fig. 9 Concentration dependence of emission intensity of Eu^{2+} and Mn^{2+} in the second series of $BaMg_2Si_2O_7$:0.006Eu^{2+}, yMn^{2+} (see text)

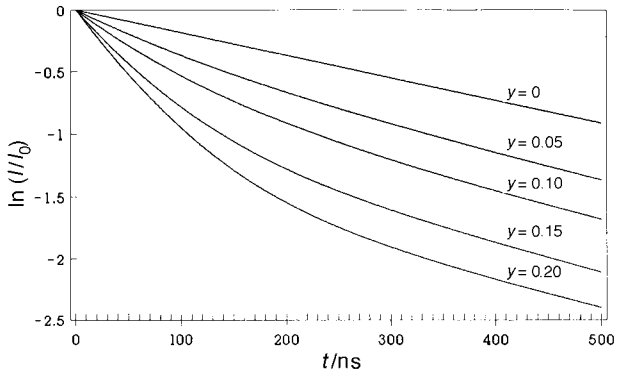

Fig. 10 Decay of the Eu^{2+} emission in $BaMg_2Si_2O_7$:0.006Eu^{2+}, $y$$Mn^{2+}$

exponential function:

$$I = I_0 \exp(-t/\tau_0) \sum_i B_i \exp(-t/\tau_i)$$

This function is related to the shell model if only the first shell is considered. From the least-squares analysis, it was found that the decay of the sample of $C_{Mn} = 0.05$ can be represented nicely with the first two terms of this function ($\tau_0 = 548$ ns and $\tau_1 = 240$ ns). This means that the single occupancy of the first shell occurs with significant probability at low Mn^{2+} doping. τ_1 is related to the energy transfer rate from Eu^{2+} to the nearest neighbor Mn^{2+} in the shell model. The decay of the samples of higher Mn^{2+} concentration (for example $C_{Mn} =$ 0.10) can be interpreted using more exponential terms with shorter decay time ($\tau_2 = 34$ ns). Although the decay times of the higher exponential terms are not exactly as expected from the shell model, it is obviously an indication that the multiple occupancy of the first shell has considerable probability at the high doping concentration. For further understanding of the energy transfer between Eu^{2+} and Mn^{2+}, studies of the low temperature spectra and the decay of Mn^{2+} are under way.

The project is supported by the National Science Foundation of China.

References

1 T. L. Barry, *J. Electrochem. Soc*., 1970, **117**, 381.
2 U. G. Caldino, A. F. Munoz and J. O. Rubio, *J. Phys.: Condens. Matter*, 1990, **2**, 6071.
3 U. G. Caldino, A. F. Munoz and J. O. Rubio, *J. Phys.: Condens. Mater*, 1993, **5**, 2195.
4 J. R. Lakowicz, in *Topics in Fluorescence Spectroscopy*, Plenum Press, New York, 1991, vol. 1, pp. 293–335.
5 G. X. Lu, J. H. Lin, G. Q. Yao and M. Z. Su, to be published.
6 G. Blasse, *Phys. Status Solidi B*, 1973, **55**, K131.
7 L. G. van Uitert, *J. Lumin*., 1971, **4**, 1.
8 C. R. Ronda and T. Amrein, *J. Lumin*., 1996, **69**, 245.
9 O. Vasquez and C. D. Flint, *Chem. Phys. Lett*., 1995, **238**, 378.
10 T. Luxbacher, H. P. Fritzer, R. Sabry-Grant and C. D. Flint, *Chem. Phys. Lett*., 1995, **241**, 103.
11 T. Luxbacher, H. P. Fritzer and C. D. Flint, *J. Phys.:Condens. Matter*, 1995, **7**, 9683.

Paper 7/05419J; *Received* 28*th July*, 1997